ECOLOGY

Phenylacetonitrile in locusts facilitates an antipredator defense by acting as an olfactory aposematic signal and cyanide precursor

Jianing Wei[1], Wenbo Shao[1,2], Minmin Cao[1,3], Jin Ge[1,3], Pengcheng Yang[1,2], Li Chen[1], Xianhui Wang[1]*, Le Kang[1,2,3]*

Many aggregating animals use aposematic signals to advertise their toxicity to predators. However, the coordination between aposematic signals and toxins is poorly understood. Here, we reveal that phenylacetonitrile (PAN) acts as an olfactory aposematic signal and precursor of hypertoxic hydrogen cyanide (HCN) to protect gregarious locusts from predation. We found that PAN biosynthesis from phenylalanine is catalyzed by *CYP305M2*, a novel gene encoding a cytochrome P450 enzyme in gregarious locusts. The RNA interference (RNAi) knockdown of *CYP305M2* increases the vulnerability of gregarious locusts to bird predation. By contrast, the elevation of PAN levels through supplementation with synthetic PAN increases the resistance of solitary locusts to predation. When locusts are attacked by birds, PAN is converted to HCN, which causes food poisoning in birds. Our results indicate that locusts develop a defense mechanism wherein an aposematic compound is converted to hypertoxic cyanide in resistance to predation by natural enemies.

INTRODUCTION

Animal aggregation occurs frequently in nature and encompasses a broad range of scales, from small groups comprising several individuals to large groups comprising millions of individuals (*1*, *2*). The benefits of aggregation include gains in foraging efficiency, shelters and mate choices, and group defense. However, aggregation also places individuals at a high risk of exposure to predators (*1*, *3*). Aposematism is a pervasive phenomenon in aggregating animals, where conspicuous and complex warning signals are used to advertise antipredator defenses (*3*–*5*). In aposematism, a warning signal is linked with toxin-induced nausea reactions to provoke aversion behaviors in predators (*4*, *6*, *7*). Warning signals can indicate the level of toxicity of an individual animal (*8*) and are positively correlated with the population density (*9*). Nevertheless, the mechanism through which gregarious prey animals coordinate the levels of warning signals and toxicity to optimize antipredator defense remains elusive.

Locusts can form large swarms, and thus, they provide fascinating model systems for studying density-dependent phase polyphenism, which involves distinct cryptic solitary and aposematic gregarious antipredator strategies. Given that defensive chemicals of the desert locust are derived from food plants, a shift from a cryptic to an aposematic strategy requires changing food sources in polyphagous locust species (*8*). The preferential consumption of toxic plants enables gregarious polyphagous locusts to acquire and accumulate distasteful chemicals, which deter predation; predators learn to avoid prey by associating the bright colors in locusts with the presence of distasteful compounds (*8*, *9*). However, oligophagous locust species, such as the migratory locust (*Locusta migratoria*), are grass specialists and are therefore unlikely to consume toxic plants (*8*, *10*). Thus, explicating the operation of conspicuous warning signals and the origin of toxic chemicals in the migratory locust remains a major challenge.

Distasteful odors can also confer noxiousness to predators and thus provide benefits for both the prey and the predator (*6*, *11*). Phenylacetonitrile (PAN; benzyl cyanide) is a major density-dependent volatile compound in locusts and may function as a conspecific communication signal in locust aggregations (*12*, *13*). Our previous study revealed that gregarious nymphs and adult males of the migratory locust can release high amounts of PAN, whereas solitary locusts cannot (*14*). Although PAN is known to serve as a growth inhibitory signal in microbe-microbe interactions (*15*, *16*) and as a repellant signal in plant-insect interactions and some other insect interactions (*17*–*19*), the role of PAN in interspecies interactions in migratory locusts has not been sufficiently investigated.

The phenylalanine metabolic pathway is responsible for the biosynthesis of PAN and its derivatives in various organisms (*20*–*23*). PAN biosynthesis begins with the conversion of phenylalanine into (*E*/*Z*)-phenylacetaldoxime [(*E*/*Z*)-PAOx] by N-monooxygenase and decarboxylase (*24*). In plants, a group of cytochrome P450 enzymes that belong to the CYP79 family participates in the catalysis of (*E*/*Z*)-PAOx synthesis (*24*–*26*). (*Z*)-PAOx is then dehydrated to PAN by the members of the CYP71 enzyme family in plants (*18*, *26*, *27*) and by (*Z*)-PAOx dehydratase in bacteria (*28*), but this is not a rate-limiting step from phenylalanine to PAN (*18*, *27*, *28*). However, to date, enzymatic evidence for PAN biosynthesis in animals remains largely unknown (*21*, *29*). PAN undergoes α-hydroxylation to generate mandelonitrile (MAN), which is further catalyzed to benzaldehyde (BA) and hydrogen cyanide (HCN) by hydroxynitrile lyase or spontaneously decomposed to BA and HCN (*30*, *31*). Despite the similarities in chemical intermediates and corresponding reaction mechanisms of the phenylalanine metabolic pathway across taxa (*23*, *28*), these pathways involve enzymes with diverse sequences (*21*). If the key biosynthetic enzyme of PAN could directly respond to the change in the population densities of locusts, then PAN biosynthesis is likely activated and regulated by a population density–dependent mechanism. Any attempt to understand the molecular mechanism of PAN biosynthesis in animal species will contribute to the functional characterization of this biologically active compound. Because PAN can be decomposed to hypertoxic

[1]State Key Laboratory of Integrated Management of Pest Insects and Rodents, Institute of Zoology, Chinese Academy of Sciences, Beijing 100080, P. R. China. [2]Beijing Institutes of Life Science, Chinese Academy of Sciences, Beijing 100101, P. R. China. [3]University of Chinese Academy of Sciences, Beijing 100049, P. R. China. *Corresponding author. Email: lkang@ioz.ac.cn (L.K.); wangxh@ioz.ac.cn (X.W.)

HCN, we hypothesize that antipredator defense systems of the migratory locust may involve PAN.

To address our hypothesis that PAN acts as a defensive agent, we combined analytical chemistry, transcriptome analysis, verification of gene function, and locust and bird bioassays to characterize the biosynthetic and metabolic pathways and the function of PAN in the migratory locust. We conclude that PAN plays a role in antipredator defense but not in conspecific aggregation. Our results reveal that an olfactory aposematic signal can be converted to a hypertoxic chemical and thereby plays an important role in shaping predator-prey interactions.

RESULTS

PAN is neither a sex-specific nor an aggregation pheromone

The function and synthetic sites of PAN may be inferred from its emission and distribution patterns. Thus, we investigated the variations in the patterns of PAN accumulation in gregarious locusts across sexes, densities, tissues, and organs. We found that sex-biased PAN production does not occur in first- to fifth-instar locust nymphs (two-tailed Student's t test: df = 10, $P > 0.05$ for each instar; Fig. 1A). PAN emission by juvenile individuals displays density-dependent changes, and the highest PAN emission per locust was observed at the highest population density [Kruskal-Wallis analysis of variance (ANOVA) on ranks test: $H = 37.138$, df = 6, $P < 0.0001$; Fig. 1B]. PAN is present in almost all tissues, organs, and body fluids (Fig. 1C and fig. S1) and is stored in considerably higher amounts in the head integument, tergum, and hind leg than in other external organs (Fig. 1C, left, and fig. S1, A and B). Fat bodies and gastric caeca exhibit higher PAN levels than other internal organs (Fig. 1C, right, and fig. S1C). Gas chromatography (GC)–mass spectrometry (MS) measurements indicated that the mean PAN amount per gregarious fourth-instar locust (G4) is approximately 130 ng [average biomass per G4 locust (300 mg) × average PAN content per unit (0.44 ng/mg)]. PAN is also the dominant volatile component of headspace volatiles and hemolymph relative to other locust volatiles, such as BA, phenol, and guaiacol (fig. S2). Overall, sex disparity in PAN production is not observed, although PAN accumulation does show tissue specificity; enriched concentrations of PAN in tissues such as the head integument, tergum, and fat body, may provide clues to the site of PAN synthesis in gregarious locusts.

We subjected gregarious fourth-instar locusts to dual-choice olfactometer tests to determine whether PAN plays an attractive role in locust aggregation. We found that gregarious nymphs significantly preferred to move and remain in the zone suffused with the odors of the paraffin oil control than in the zone suffused with PAN at or above the dosage equivalent of 10 locust emission minutes (LMs) [Wilcoxon signed rank test: total distance moved in Fig. 1D, $Z = 4.26$, $P < 0.001$ (for control versus 1000 LM); $Z = 3.21$, $P = 0.001$ (for control versus 200 LM); $Z = 3.35$, $P < 0.001$ (for control versus 10 LM); $Z = 1.65$, $P = 0.101$ (for control versus 1 LM); time in zone in Fig. 1E, $Z = 4.49$, $P < 0.001$ (for control versus 1000 LM); $Z = 3.46$, $P < 0.001$ (for control versus 200 LM); $Z = 3.22$, $P = 0.001$ (for control versus 10 LM); $Z = 1.36$, $P = 0.18$ (for control versus 1 LM)]. Thus, gregarious locusts do not display attraction to PAN at various dosages, excluding PAN from participation in locust aggregation.

(*E*/*Z*)-PAOx is only produced by gregarious locusts

(*Z*)-PAOx is a precursor of PAN in the phenylalanine metabolic pathway. Thus, we conducted the biochemical analysis of (*Z*)-PAOx and its trans isomer (*E*)-PAOx in hexane extracts from tissues and organs in gregarious and solitary locusts. Our GC-MS/MS multiple reaction monitoring (MRM) results revealed that (*E*/*Z*)-PAOx is produced in gregarious locusts but not in solitary locusts (Fig. 2A). Moreover, the distribution pattern of (*Z*)-PAOx indicates that (*Z*)-PAOx is produced exclusively in the integuments (Fig. 2B). However, we failed to detect (Z)-PAOx in other tissues, organs, fat bodies, and

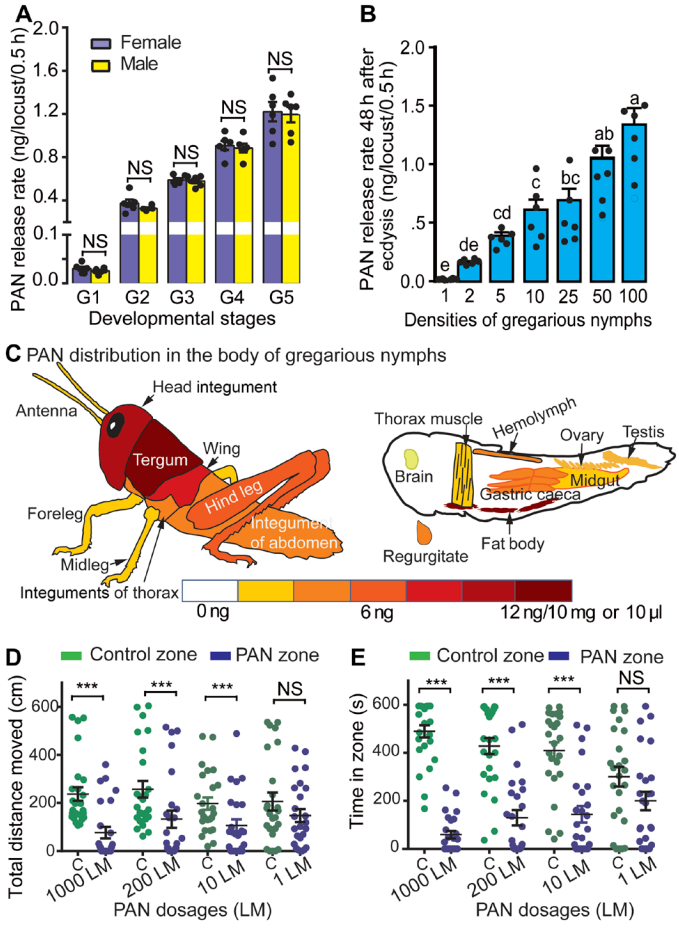

Fig. 1. PAN production patterns and behavioral responses of gregarious locusts under treatment with different dosages of synthetic PAN. (**A**) PAN production by first-instar (G1) to fifth-instar (G5) nymphs (means ± SEM, six biological replicates per sex per developmental stage, $n = 6$). Data for the two sexes were compared using two-tailed Student's t test. (**B**) PAN emission per nymph reared under different population densities (1 to 100 nymphs). Data were analyzed using Kruskal-Wallis ANOVA on ranks following Tukey honestly significant difference (HSD) post hoc test. Different letters above bars represent significant differences among densities [$P < 0.05$ (means ± SEM, $n = 6$ biologically independent samples)]. (**C**) Whole-body PAN production by a gregarious locust. Detailed statistical analyses are shown in fig. S1. (**D**) Total distance moved (in centimeters) of a fourth-instar gregarious locust in the PAN zone versus in the paraffin oil control zone over 10 min in the dual-choice bioassay. (**E**) Total time spent (in seconds) over 10 min in the PAN zone versus that in the control zone. (D and E) PAN dosages used in behavioral assays were expressed as LM (1 LM = PAN emitted by one locust over 10 min in the PAN zone of the observation arena; dosages from 1 LM to 1000 LM; for a detailed description, see Materials and Methods). Under each treatment dosage, 25 locusts successfully finished the dual-choice tests ($n = 25$); C, control treatment. Distance or time data in the PAN zone versus the control zone for every treatment dosage were compared using Wilcoxon signed rank test (***$P < 0.001$; NS, not significant). All data are presented as the means ± SEM.

body fluids of gregarious locusts (table S1). These results suggest that phenylalanine is enzymatically converted into (*E*/*Z*)-PAOx in the integument. In addition, (*E*/*Z*)-PAOx is a gregarious locust-specific chemical involved in PAN biosynthesis.

CYP305M2 is responsible for PAN biosynthesis

Given that PAN biosynthesis from phenylalanine involves a member of the cytochrome P450 family in plants and bacteria (*24*–*26*), we predicted that cytochrome *P450* genes may participate in PAN biosynthesis in gregarious locusts. After analyzing the RNA sequencing (RNA-seq) data of the migratory locust, we found that among the 122 identified *CYP* genes, 4 are consistently up-regulated in gregarious locusts relative to that in solitary locusts in all stages (fig. S3A). The knockdown of these putative genes through double-stranded RNA (dsRNA)–mediated RNA interference (RNAi) demonstrates that, although all four candidate genes are effectively down-regulated (Kruskal-Wallis ANOVA on ranks test: $H = 11.18$, df = 2, $P = 0.004$; Fig. 2C and fig. S4, A to C), only the RNAi knockdown of *CYP305M2* (*LM16181* shown in fig. S3B) specifically reduces (*Z*)-PAOx and PAN production in gregarious locusts to levels comparable with those in solitary locusts [Kruskal-Wallis ANOVA on ranks test: $H = 11.18$, df = 2, $P = 0.004$ for PAN and $H = 13.29$, df = 2, $P = 0.001$ for (*Z*)-PAOx; Fig. 2, D and E, and fig. S4D]. Amino acid sequence analyses revealed that *CYP305M2* is closely related to the members of the CYP305A subfamilies from other insect species (fig. S5). The expression pattern of *CYP305M2* (fig. S6) corresponds with the release pattern of (*Z*)-PAOx. This finding indicates that CYP305M2 participates in (*Z*)-PAOx biosynthesis. The results for the immunohistochemical analysis of head integument tissue slides reveal that CYP305M2 is expressed only in the oenocytes of gregarious locusts (Fig. 2F and fig. S7). This result thus confirms that *CYP305M2* is specifically involved in the PAN pathway.

CYP305M2 is a rate-limiting and density-dependent enzyme

To further confirm whether the biosynthesis of cyanogenic aldoxime and nitrile differs between solitary and gregarious locusts, we injected

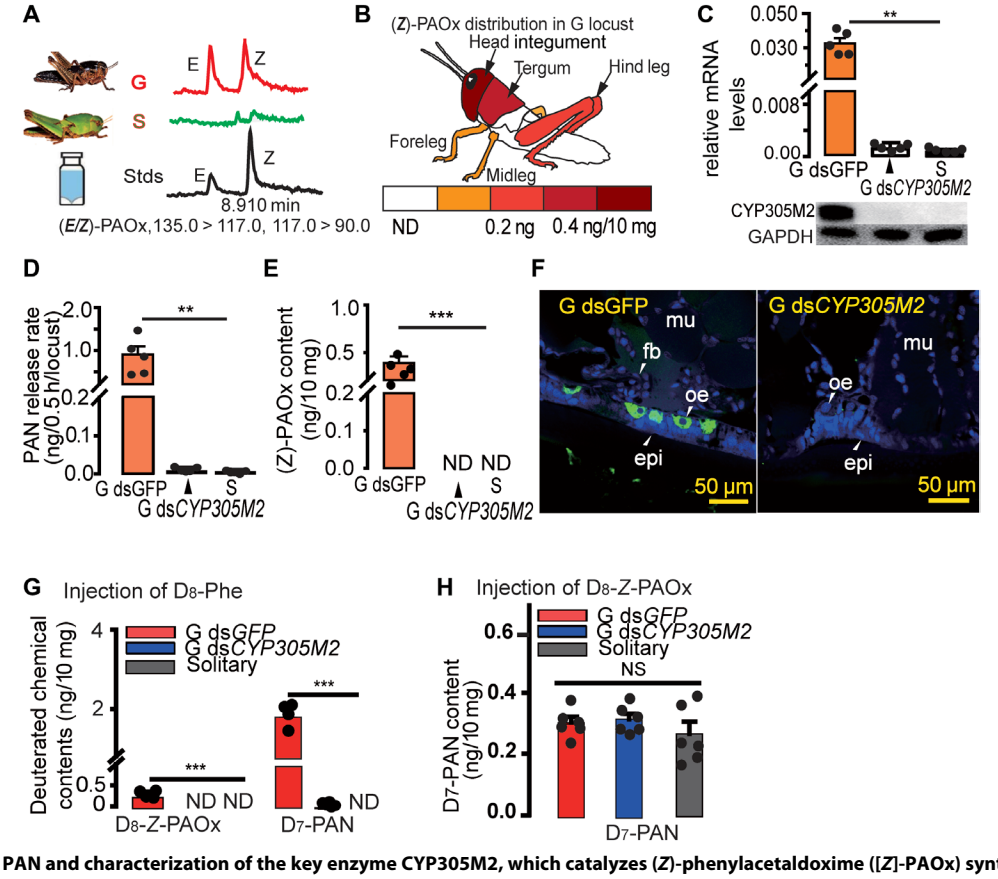

Fig. 2. Biosynthesis of PAN and characterization of the key enzyme CYP305M2, which catalyzes (*Z*)-phenylacetaldoxime ([*Z*]-PAOx) synthesis in the migratory locust. (**A**) GC-MS MRM chromatograms of (*E*/*Z*)-PAOx in the head integuments of gregarious (G, red trace) and solitary (S, green trace) locusts and synthetic standards (stds, black trace). (*E*/*Z*)-PAOx was identified on the basis of the chemical parent (135) and daughter ions (117 and 90). (**B**) (*Z*)-PAOx distribution in the body of a gregarious locust. Detailed statistical analyses are presented in table S1. (**C** to **E**) *CYP305M2* expression (relative to *rp49* gene), protein level (relative to GAPDH), and PAN and (*Z*)-PAOx production in head integument tissues of gregarious locusts at 48 hours after dsRNA injections and in those of untreated solitary locusts. Data were analyzed using Kruskal-Wallis ANOVA on ranks following Tukey HSD post hoc test (**$P < 0.01$, ***$P < 0.001$; means ± SEM, $n = 5$ biologically independent samples for each bar). (**F**) Histological localization of CYP305M2 in head integument tissue from dsGFP-injected (left) and ds*CYP305M2*-injected (right) gregarious locusts. CYP305M2 protein was detected in oenocytes (arrowheads). oe, oenocytes; epi, epidermal cell; fb, fat body; mu, muscle. Green, CYP305M2; blue, nuclear. Scale bars, 50 μm. (**G**) D_8-Phe incorporation into (*Z*)-PAOx and PAN in dsGFP- or ds*CYP305M2*-injected gregarious and untreated solitary locusts. Data were analyzed using Kruskal-Wallis ANOVA on ranks following the Tukey HSD post hoc test (***$P < 0.001$; means ± SEM, $n = 4$ biologically independent samples). (**H**) Incorporation of deuterium-labeled (*Z*)-PAOx incorporation into PAN in dsGFP- or ds*CYP305M2*-injected gregarious locusts and untreated solitary locusts. ANOVA test (ND, not detected; means ± SEM, $n = 6$ biologically independent samples).

deuterium-labeled L-phenyl-D_5-alanine-2,3,3-D_3 (D_8-Phe) into the abdomens of the double-stranded green fluorescent protein (dsGFP)– or ds*CYP305M2*-injected gregarious locusts or untreated solitary locusts. The amounts of deuterium-incorporated D_8-(*Z*)-PAOx and D_7-PAN in the head integument extracts of dsGFP-injected locusts are consistently and significantly higher than those in the head integument extracts of ds*CYP305M2*-injected and solitary locusts [Kruskal-Wallis ANOVA on ranks test: $H = 10.45$, df = 2, $P = 0.015$ for D_8-(*Z*)-PAOx and $H = 10.23$, df = 2, $P = 0.001$ for D_7-PAN; Fig. 2G]. This result provides direct evidence that *CYP305M2* is a (*Z*)-PAOx–specific CYP gene and encodes a crucial rate-limiting enzyme in PAN biosynthesis in gregarious locusts. However, D_7-PAN is present in all D_8-(*Z*)-PAOx–injected locusts at concentrations that are not significantly different across treatments (ANOVA, $F_{2,15} = 0.731$, $P = 0.498$; Fig. 2H). These outcomes indicate that the absence of PAN in solitary locusts mainly results from the unavailability of (*Z*)-PAOx, which is activated by a high population density of locusts.

PAN is an olfactory aposematic signal to bird predators

The body coloration (Fig. 3A) and volatile blend composition (Fig. 3B) of gregarious locusts are markedly different from those of solitary locusts. We attempted to examine the aposematic role of body coloration and volatile blend composition in the predatory defense of locusts against the great tit (*Parus major*), a common insectivorous bird species distributed throughout Europe and Asia (*32*). The results of a dual-choice bioassay show that, under light and dark conditions, the great tit preferentially selects and feeds on solitary over gregarious locusts (Supplementary Text, fig. S8, and movies S1 and S2). These findings suggest that a characteristic other than body color signals the distastefulness of gregarious locusts to great tits. Given that PAN is the most important volatile component that contributes to the difference between the volatile compositions of gregarious and solitary locusts (*14*), we assume that PAN may act as an olfactory aposematic signal in locusts.

To test whether PAN production by locusts influences predation by the great tit, we performed a series of dual-choice and predation tests involving locusts with or without PAN load. First, we perfumed solitary locusts with synthetic PAN without changing other major volatile components (fig. S9). We found that great tits refused to attack and feed on PAN-treated solitary locusts [Wilcoxon signed rank test: $Z = 2.64$, $P = 0.008$ (for first choice); $Z = 2.701$, $P = 0.004$ (for injury rate); $Z = 2.66$, $P = 0.004$ (for consumption rate); $n = 9$ birds; Fig. 3C and movie S3]. Second, we confirmed the specific role of PAN in great tit selection and predation through a knockdown experiment by injecting ds*CYP305M2* and dsGFP into gregarious locusts. The *CYP305M2* knockdown through RNAi allows the specific elimination of PAN from the experimental prey without interfering with other chemical and body color characteristics (fig. S10). We found that ds*CYP305M2*-injected locusts are frequently attacked and are preferentially consumed by great tits over dsGFP-injected or PAN-treated ds*CYP305M2*-injected locusts [Wilcoxon signed rank test: ds*CYP305M2*-injected versus dsGFP-injected locusts: $Z = 2.95$, $P = 0.001$ (for first choice); $Z = 3.089$, $P = 0.001$ (for injury rate); $Z = 3.059$, $P = 0.001$ (for consumption rate); $n = 12$ birds; Fig. 3D; PAN-treated versus hexane-treated ds*CYP305M2*-injected locusts: $Z = 2.588$, $P = 0.008$ (for first choice); $Z = 2.812$, $P = 0.002$ (for injury rate); $Z = 2.803$, $P = 0.002$ (for consumption rate); $n = 10$ birds; Fig. 3E and movies S4 and S5]. Furthermore, we observed that injury rates of PAN-treated beetle mealworms *Tenebrio molitor*, a major

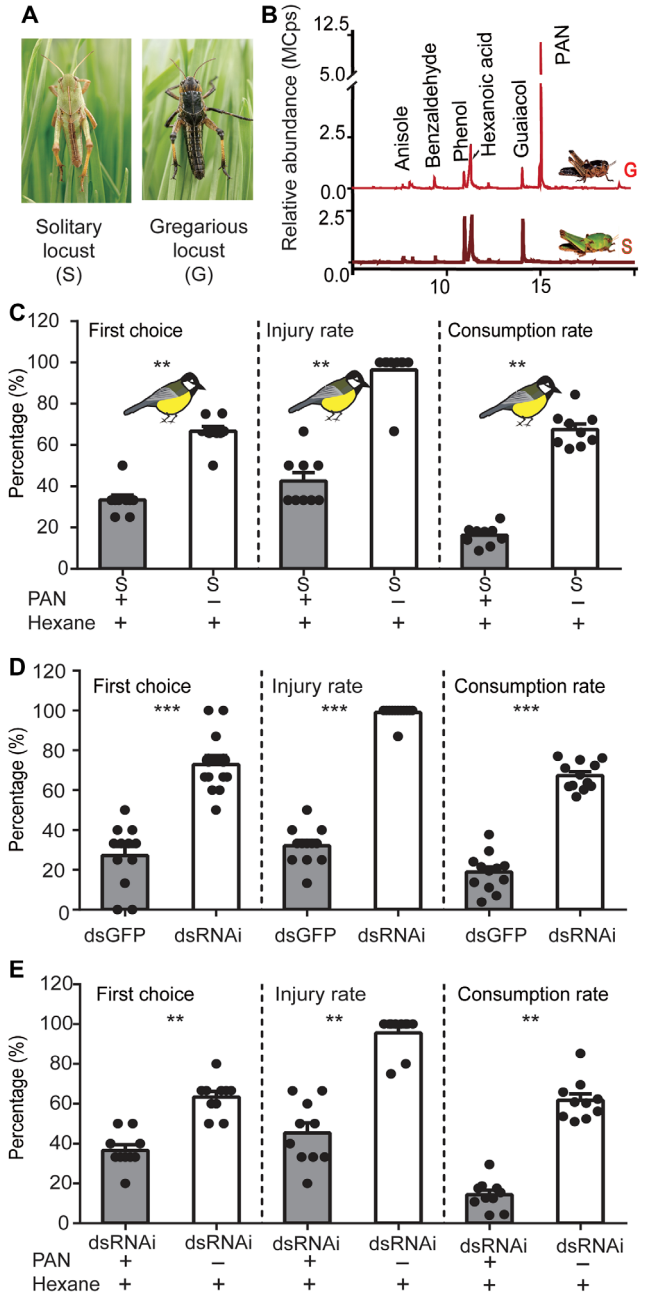

Fig. 3. PAN emission by the migratory locust influences predation by the great tit. (**A**) Typical gregarious and solitary fourth-instar nymphs on a background of green plants. Photo credit: All authors. (**B**) Total ion GC-MS chromatograms of SPME-trapped headspace volatiles of fourth-instar gregarious (G) (red trace) and solitary (S) (green trace) locusts. Major locust volatiles are listed above the compound peaks. PAN is present as the most abundant component in gregarious locusts but is absent from solitary locusts. (**C**) In a dual-choice bioassay conducted with paired locusts, the percentage (%) of the great tits selected and fed on hexane-treated solitary locusts (control) or PAN-treated solitary locusts. The first choice, injury rate, and consumption rate of the locusts by the great tits are recorded (means ± SEM, $n = 9$ birds). (**D**) First choice, injury rate, and consumption rate for the paired dsGFP-injected gregarious locusts and ds*CYP305M2* (dsRNAi)–injected gregarious locusts (means ± SEM, $n = 12$ birds). (**E**) Selections of great tits between a hexane-treated ds*CYP305M2*-injected locust (control) and a PAN-treated ds*CYP305M2*-injected locust (right) (means ± SEM, $n = 10$ birds). (C to E) Paired data were compared using Wilcoxon signed rank test. $^{**}P < 0.01$, $^{***}P < 0.001$.

component of the great tit diet, decreased by 90% relative to that of hexane-treated beetle mealworms (fig. S11). In addition, BA and phenol, two other major locust volatiles, do not affect the rates of locust predation by great tits (fig. S12). Thus, our result indicates that PAN produced by gregarious locusts reduces bird predation and serves as an olfactory aposematic signal in locust defense.

PAN is converted to HCN in attacked locusts

PAN is a chemical precursor of HCN, a common toxin against vertebrates and invertebrates (*20*). To determine whether the aposematic role of PAN in gregarious locusts can be attributed to the conversion of PAN to the hypertoxic HCN, we performed GC-MS to determine the presence of HCN in the locust. The results show that HCN concentrations in the headspaces of vials containing undisturbed gregarious or solitary locusts are relatively low and do not differ from each other (Mann-Whitney *U* test: $Z = 0.88$, $P = 0.394$; Fig. 4A and fig. S13A). However, the amounts of HCN released by gregarious locusts under attack by great tits are 11-fold higher than that released by undisturbed gregarious locusts (Mann-Whitney *U* test: $Z = -2.8$, $P = 0.005$; Fig. 4A and fig. S13B). To mimic bird attacks, we used a vortex mixer to shake locusts that were confined in vials (for the detailed rationale for this method, see Materials and Methods and movie S6). We found that the amounts of HCN released by shaken gregarious locusts are 14-fold higher than that released by undisturbed gregarious locusts (Mann-Whitney *U* test: $Z = 2.9$, $P = 0.003$; Fig. 4A and fig. S13C). To determine whether a causal link exists between PAN and HCN production in locusts, we measured the HCN emissions after the RNAi knockdown of *CYP305M2* in gregarious locusts or in PAN- and (Z)-PAOx–supplemented solitary locusts. Notably, disturbed ds*CYP305M2*-injected locusts release lower amounts of HCN than disturbed dsGFP-injected locusts (fig. S13D). Disturbed PAN-injected solitary locusts also release significantly higher amounts of HCN than control solitary locusts (Kruskal-Wallis ANOVA on ranks test: $H = 26.91$, df = 4, $P = 0.0001$; Fig. 4B and fig. S13E).

PAN is also a chemical precursor of BA; thus, we predicted that BA should also increase in response to population density and mechanical disturbance in locusts. Our high-performance liquid chromatography (HPLC) analyses show that BA is present at consistently and significantly higher amounts in dsGFP-injected gregarious locusts than in ds*CYP305M2*-injected gregarious locusts or solitary locusts under undisturbed and disturbed (from shaking) conditions (Kruskal-Wallis ANOVA on ranks test: $H = 15.72$, df = 2, $P = 0.0001$ under undisturbed condition and $H = 15.17$, df = 2, $P = 0.0001$ under disturbed condition; Fig. 4C and fig. S14, A and B). BA production in mechanically disturbed dsGFP-injected gregarious locusts is remarkably elevated compared with that in undisturbed gregarious locusts (two-tailed Student's *t* test: df = 10, $P < 0.0001$; Fig. 4C). We further validate, by injecting D_8-Phe into locusts, that D_6-BA production occurs in locusts through the phenylalanine metabolic pathway (Fig. 4D).

In brief, when the locusts are attacked by birds or disturbed by shaking, PAN can be converted to hypertoxic HCN, indicating that PAN can advertise HCN toxicity to predators.

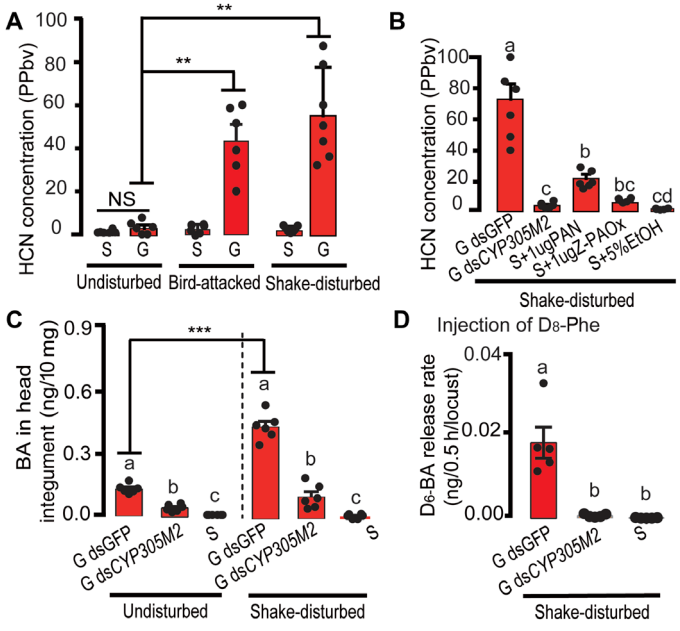

Fig. 4. HCN biosynthesis from PAN in gregarious locusts. (**A**) HCN production in the headspaces of vials containing intact undisturbed, bird-attacked, or shake-disturbed (SD) gregarious and solitary locusts in the fourth-instar stage at 48 hours after ecdysis. Data were compared using Mann-Whitney *U* test (means ± SEM, $n = 6$ biologically independent samples for intact and bird-attacked locusts and $n = 7$ for SD locusts; $^{**}P < 0.01$). (**B**) HCN contents of the headspaces of vials containing SD gregarious locusts injected with dsGFP or ds*CYP305M2* and solitary locusts injected with PAN (1 μg per locust), (*Z*)-PAOx (1 μg per locust), and solvent control (10 μl of 5% EtOH per locust). Data are expressed as the means ± SEM ($n = 6$ biologically independent samples). (**C**) BA production in the head integument of intact undisturbed or SD fourth-instar dsGFP- or ds*CYP305M2*-injected gregarious (G) and solitary (S) locusts at 48 hours after ecdysis. Data are expressed as the means ± SEM ($n = 6$ biologically independent samples). (**D**) D_8-Phe incorporation into BA in the headspace of SD dsGFP- or ds*CYP305M2*-injected gregarious and solitary locusts. Data are expressed as the means ± SEM ($n = 5$ biologically independent samples). (B to D) Data were statistically analyzed through Kruskal-Wallis ANOVA by ranks following Tukey HSD post hoc test. Different letters show significant differences among treatments ($P < 0.05$). (C) BA production levels by intact and SD dsGFP-injected gregarious locusts were compared using two-tailed Student's *t* test ($^{***}P < 0.001$).

DISCUSSION

Our results indicate that PAN does not play a role in the aggregation of the migratory locust in the nymphal stage. In gregarious locusts, the PAN and HCN biosynthetic pathways participate in an antipredator defense mechanism that involves the coordination of olfactory aposematism and chemical defense (Fig. 5). The activation of a crucial *CYP* gene in the phenylalanine metabolic pathway during locust aggregation is an important mechanism in the adaptation of gregarious locusts to the group-living environment. There are many insectivorous bird species including seasonal migratory and nonmigratory birds in the field, so the aggregation exposures of the locusts obviously have the higher risks of predations. Because the activation of the PAN biosynthesis relies on the high population density of the locusts, the chemical defense of the locusts aims at the general predators in spite of the great tit being used in the behavioral tests. Thus, the plasticity of PAN biosynthesis in response to population density is crucial for the optimization of the antipredator defense strategies of locusts under diverse environmental conditions.

We identified a novel gene member of the cytochrome P450 family that catalyzes the biosynthesis of PAN from phenylalanine in animals. We found that the conversion of phenylalanine to (*Z*)-PAOx by

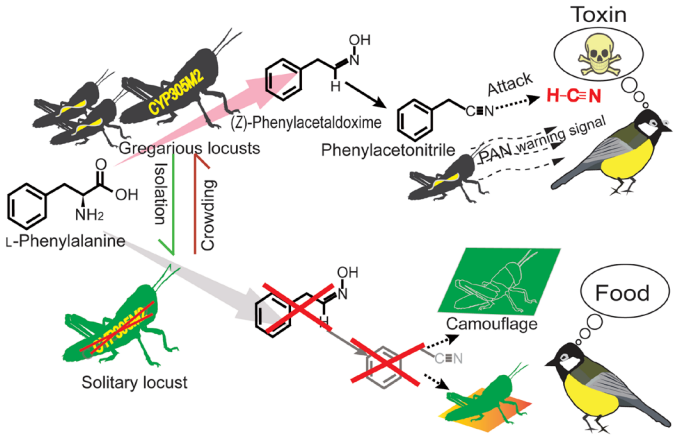

Fig. 5. Model of the biosynthesis of PAN and HCN from phenylalanine, the steps of cyanogenesis, and the responses of bird predators to gregarious and solitary locusts. A cytochrome (CYP) gene (*CYP305M2*) that catalyzes the formation of (*Z*)-PAOx, a precursor in PAN and HCN biosynthesis from phenylalanine in gregarious locusts, was identified. *CYP305M2* is present at barely detectable levels in solitary locusts. Aposematism with PAN can warn and deter consumers from poisoning by HCN generated from PAN. The yellow marker in gregarious locusts denotes the expression of *CYP305M2*. Against a green background, solitary locusts use camouflage to appear cryptic to predators and are otherwise readily discovered and predated.

CYP305M2 is the rate-limiting step in the PAN pathway in locusts. This substrate-specific and rate-limiting step is also involved in the synthesis of (*Z*)-PAOx from phenylalanine in plants (*24*–*26*). Although phenylalanine N-hydroxylation and decarboxylation are conserved across all organisms, the gene involved in these reactions differs across species (*18*, *24*–*28*, *33*). Thus, identifying the putative enzymes that participate in PAN production on the basis of similarities with known sequences is difficult. We used transcriptome analysis and RNAi to identify the rate-limiting *P450* gene. Our research system enables the identification and verification of the candidate genes responsible for PAN production in an animal species. The enzymatic conversion of (*Z*)-PAOx to PAN by aldoxime dehydratases, which are CYP71s with a broad range of substrates that participate in aldoxime metabolism in cyanogenic plants (*18*, *27*), does not differ between gregarious and solitary locusts. Considering the high PAN–to–(*Z*)-PAOx ratio (approximately 20:1) of gregarious locusts, we inferred that this step is not the rate-limiting reaction in PAN biosynthesis. Through deuterium labeling coupled with GC-MS/MS MRM analysis, we found that the conversion of phenylalanine to BA and HCN is an important step in cyanogenesis in locusts. Although the phenylalanine metabolic pathway involves chemical intermediates and corresponding reaction mechanisms that are relatively similar across taxa from prokaryotic microorganisms to higher eukaryotes, it also includes enzymes with markedly divergent sequences (*21*, *23*, *28*). Thus, highly sensitive and state-of-the-art techniques should be considered and used to further investigate the molecular mechanisms underlying the other steps of the PAN pathway in animals. Our RNAi experiment showed that *CYP305M2* knockdown can specifically eliminate PAN emission without interfering with the production of other volatiles and the expression of morphological characteristics in RNAi-treated gregarious locusts relative to those in GFP-treated individuals. Thus, this powerful tool can provide novel insight into the actual functions of PAN in other locust species. For example, the identification of the homologous *CYP305M2* gene and observations on the aggregation and courtship behaviors of gene-manipulated locusts will greatly elucidate the function of PAN as either an aggregation pheromone (*34*) or a courtship inhibition pheromone (*19*). This approach may promote clarity of understanding and resolve the long-standing controversy of the "PAN paradox" in locusts (*13*).

As an aposematic signal, PAN can prevent consumers from being poisoned by HCN generated from PAN in the bodies of prey animals and can warn consumers of the risk of the metabolic conversion of PAN to cyanide in the bodies of the consumers (*35*). Birds most likely evolved an innate aversion to PAN to avoid poisoning by HCN, which is only produced in large quantities in attacked gregarious locusts (Fig. 4A). Thus, we confirmed our hypothesis that PAN participates in antipredator defense in locusts by acting as an aposematic olfactory signal and toxin precursor. This finding provides an alternative case for the theoretical concept of olfactory aposematism proposed by Eisner and Grant (*11*) and partially supports the results of a recent empirical study on the role of conditioned aposematic volatiles in marine environments (*36*). Although avoidance learning allows predators to reject prey animals after detecting distastefulness (*2*), learning becomes problematic when prey animals, such as cyanogenic species, become extremely toxic and even lethal (*23*). In this regard, predators are given no chance to learn from their mistakes (*37*). Thus, olfactory aposematism through pyrazine (*38*) or PAN emission can warn predators of the presence of toxic compounds (*39*) and thereby induce innate avoidance behavior (*11*). This strategy benefits predators and prey animals because the optimized defense strategy of prey animals is to avoid predators during the early stages of the predator-prey interaction.

We demonstrated for the first time that gregarious migratory locusts can produce HCN. Given this characteristic, the migratory locust is a cyanogenic insect species. Cyanogenesis is an important defense mechanism of many plants and arthropods because HCN is an extremely fast-acting broad-spectrum toxin (*23*, *40*). Cyanogenic prey animals have to coordinate HCN biosynthesis, storage, and mobilization to prevent self-poisoning by HCN and to facilitate defense. Ordinarily, cyanide is stored in the form of cyanogenic glucosides and cyanohydrins in cyanogenic glands (*20*, *23*, *41*). Upon tissue damage or stress, these cyanogenic compounds are hydrolyzed or decomposed to liberate HCN (*21*, *41*, *42*). By contrast, gregarious locusts store HCN in the form of PAN, which is more stable than other cyanogenic intermediates, such as (*Z*/*E*)-PAOx and MAN, in all tissues and organs. PAN, an irritant, acts as the first line of defense against predation by warning predators of the potential toxicity of the prey. Otherwise, PAN is rapidly converted to HCN. In this study, we have revealed the sequential functional coordination between a warning signal and a toxin to facilitate self-protection and defense in a cyanogenic prey. Nevertheless, the mechanism of this strategy requires further investigation. Despite the effectiveness of cyanogenesis as a defense mechanism, the longevity and fecundity of gregarious locusts are lower than those of solitary locusts (*43*, *44*). These characteristics may be attributed to the high cost of PAN maintenance. The cost of PAN production may also explain why solitary locusts merely use cryptic camouflage instead of combining PAN production with camouflage for antipredator defense. However, this hypothesis needs further investigation.

Our finding regarding the aposematic role of PAN in the nymphal stages provides a new point in the discussion on the role of PAN in

adult locusts. Mature adult males in both gregarious desert locust and migratory locust release higher amounts of PAN than nymphs (*14*, *45*) and can also transfer PAN to females during copulation for postcopulatory mate guarding (*29*). Thus, our results may suggest that gregarious adult males can also use PAN for antipredator defenses. Exploring whether adult female locusts can also use PAN obtained during copulation in defense is likewise an interesting topic for future study.

In summary, our results reveal an unprecedented antipredator mechanism in the migratory locust. PAN has a dual role in antipredator defense as an honest olfactory aposematic signal and as an indicator of HCN toxicity. The dual roles of PAN increase the resistance of gregarious locusts to predation. The increased predator resistance of locusts, in turn, likely contributes to the development of locust swarms. Genetic engineering strategies for the biological control of locust populations may target the *CYP* gene that encodes for the rate-limiting enzyme in PAN biosynthesis to eliminate the defense mechanisms of gregarious locusts.

MATERIALS AND METHODS

Experimental animals

The migratory locust (*L. migratoria*) used in the experiments was reared as reported by Wei *et al.* (*14*). Briefly, the gregarious locusts were cultured in cages (30 cm × 30 cm × 30 cm) at densities of 800 to 1000 first-instar insects per cage in a well-ventilated insectary room. The solitary locusts were individually reared in a ventilated cage (10 cm × 10 cm × 25 cm) in another insectary room. All colonies were reared at L14:D10 photoperiod, 30° ± 2°C temperature, 60 ± 5% relative humidity, and on a diet of fresh greenhouse-grown wheat seedlings and bran.

Wild great tits (*P. major*) were caught in mist nets near Fangshan Country, Beijing (39°46′54″ N, 115°57′17″ E). This insectivorous bird is a common species throughout Europe and Asia (*32*). Birds were housed individually in 0.3-m^3 birdcages and were reared at L14:D10 photoperiod, 25° ± 2°C temperature, 60 ± 5% relative humidity, and on a diet of commercially available living mealworms (*T. molitor*) and millets. All birds were acclimated to the laboratory environment, facilities, and researchers for 2 to 4 weeks, during which they had no experiences with the migratory locust and their odors before the experiments. After the experiments, they were released to the places where they were mist-netted. All experiments were conducted under the license of the Animal Experimental Committee of the Institute of Zoology (AECIOZ), Chinese Academy of Science (IOZ20170071).

Chemicals

Ultrapure water was produced by a Milli-Q system (Millipore, Bedford, MA, USA). PAN, MAN, and other locust volatile standards (purities ≥ 95%) were purchased from Sigma-Aldrich (St. Louis, MO, USA). HPLC-MS grade hexane, ethanol (EtOH), acetonitrile (ACN), and methanol (MeOH) were obtained from Thermo Fisher Scientific UK (Geel, Belgium). [Ring-D5, 2,3,3-D3]-phenylalanine (D_8-Phe) and [Ring-D5, 2-D1]-phenylaldehyde (D_6-BA) were purchased from Cambridge Isotope Laboratories Inc. (Andover, MA, USA). Other chemicals and reagents were of the highest grade unless otherwise specified.

(*E*/*Z*)-PAOx and [Ring-D5, 2,3,3-D3]-(*E*/*Z*)-phenylacetaldoxime [D_8-(*E*/*Z*)-PAOx] were synthesized according to a protocol provided in a previous report (*18*). In brief, 200 mg of phenylalanine (Phe) or D_8-Phe was dissolved in 20 ml of 1 M sodium carbonate solution, which was saturated with mannitol and NaCl and adjusted to pH 10 with 0.2 N NaOH solution. Toluol (100 ml) was added to the mixture. Freshly prepared 0.5% NaOCl solution (200 μl) saturated with NaCl was added to the reaction mixture every 2 min under magnetic stirring until a total of 12 ml was added. Toluol was replaced every 12 min, and the combined toluol extracts were dried with sodium sulfate overnight. Hydroxylamine hydrochloride solution [100 mM (pH 7) and 30 ml] was added, and the mixture was then stirred at room temperature for 1 hour. The toluol layer was separated and dried with sodium sulfate. The solvent was evaporated to yield a solid product. The product identities were verified by ^{1}H-NMR and GC-MS (figs. S15 and S16; detailed methods are in the "Chemical analysis and quantification" section). The GC-MS peak areas revealed that the (*E*/*Z*)-PAOx product contains PAN (8%), (*E*)-PAOx (24%), and (*Z*)-PAOx (68%) (fig. S15B), and the D_8-(*E*/*Z*)-PAOx product contains D7-PAN (9.9%), D_8-(*E*)-PAOx (40%), and D_8-(*Z*)-PAOx (50.1%) (fig. S16A). Thus, the D_7-PAN and *Z*-isomers of aldoximes were purified by HPLC on an Agilent 1260 infinity HPLC system (Agilent Technologies), equipped with CHIRALPAK AD-H (250 × 4.6 mm; Daicel Chiral Technologies Co. Ltd., Shanghai, China). Chromatograms were recorded using an ultraviolet (UV) detector at λ = 210 nm. Throughout the HPLC programming, isocratic elution with 95% hexane and 5% isopropanol was run for 15 min at a flow rate of 1 ml min^{-1}, with the column maintained at 25°C. The effluent fractions of D_7-PAN [retention time (RT), 7.2 min] and *Z*-isomers of aldoximes (RT, 11.8 min) were separately collected in glass vials (20-ml headspace vial, Agilent Technologies; fig. S17). Approximately 15 ml of each collected compound was evaporated to dryness under a gentle stream of nitrogen gas on ice, and 100 μl of EtOH was added into each dried residue. For quantification, 2 μl of EtOH-dissolved residue was further diluted 100-fold by hexane. Synthetic PAN (Sigma-Aldrich) in different dosages (1, 5, 10, 50, and 100 ng/μl in hexane) was used as an external standard to develop the standard curves to quantify the D_7-PAN and aldoximes in diluted residue by the GC-MS method described below. A certain volume of EtOH was added into each 98-μl EtOH dissolved residue to form a primary stock (2 mg/ml). The D_8-(*Z*)-PAOx stock was further diluted to a certain concentration by ultrapure water for experiments of in vivo conversion of aldoxime to nitrile in locusts.

Experimental designs and chemical extractions

PAN and (E/Z)-PAOx accumulation in gregarious locusts

The emission and distribution patterns of PAN and its precursor (*E*/*Z*)-PAOx may reflect their synthetic sites and function. Thus, we first investigated the variations in the accumulation patterns of these compounds in gregarious locusts across sexes, densities, tissues, and organs.

To determine differences between the levels of headspace PAN released by female and male nymphs in the first to fifth instars (Fig. 1A), gregarious locusts were cultured in Perspex cages (10 cm × 10 cm × 10 cm) at densities of 50 individuals. To determine the level of PAN emissions by fourth-instar nymphs (Fig. 1B), gregarious locusts were cultured at densities of 1 to 100 individuals in Perspex cages (15 cm × 15 cm × 11 cm). To determine differences between PAN production by locusts treated with the dsRNA of GFP and *CYP305M2* (Fig. 2D), gregarious fourth-instar nymphs from a cultured colony were injected with ds*CYP305M2* and dsGFP immediately after

ecdysis. The detailed methodology for preparation of the ds*CYP305M2* and dsGFP is described below. The colonies of ds*CYP305M2*- and dsGFP-injected locusts in the fourth-instar nymphal stage were maintained in gregarious rearing cages (Perspex boxes, 15 cm × 15 cm × 11 cm), as previously described.

The headspace PAN of locusts was extracted via static solid-phase microextraction (SPME) in accordance with a previously described method by Wei *et al.* (*14*). Polydimethylsiloxane/divinylbenzene fibers (65 μm; Supelco, Bellefonte, USA) were introduced into glass jars (10.5 cm height × 8.5 cm internal diameter) containing a group of 10 nymphs in the first or second instar or individual locusts in the third to fifth instar from different colonies. The fiber was exposed for 30 min to the headspace of locusts. A clean glass jar without a locust served as the control. All locusts were subjected to the SPME system for PAN absorption at 48 hours after hatching or at 48 hours after ecdysis.

PAN and (*E*/*Z*)-PAOx were extracted from different locust tissues or organs through solvent absorption (Figs. 1C and 2, B and E; fig. S1, A to C; and table S1). Solitary or gregarious fourth-instar locusts at 48 hours after ecdysis were used in all experiments. Gregarious locusts were obtained from the colonies of dsGFP-injected, ds*CYP305M2*-injected, or three other dsRNAs-injected locusts (table S2) reared at a density of 100 individuals in gregarious rearing cages (Perspex boxes, 15 cm × 15 cm × 11 cm). Approximately 10 to 100 mg of fresh tissue samples were transferred into a 1.5-ml Eppendorf tube containing 0.2 ml of ultrapure water and homogenized thoroughly for 30 to 60 s with an electric pestle (Kontes, Vineland, NJ). Integument tissues were homogenized in liquid nitrogen. Hexane (200 μl) containing 4 ng of 4-methyl PAN (4Me-PAN) was added to each sample as an internal standard. The samples were agitated for 10 min at 4°C and then centrifuged at 13,000 rpm for 10 min. The upper layer of the hexane phase was subsequently transferred to a 150-μl insert tube in a 2-ml screw cap vial (Waters Co., USA) with Teflon/rubber septa and stored at −20°C until further analysis. For the extraction of PAN from locust hemolymph or regurgitate (fig. S1D), 30 to 50 μl of hemolymph or regurgitant obtained from five locusts of the same cohort were added into an Eppendorf tube containing 200 μl of hexane with 4 ng of the internal standard 4Me-PAN. Hexane extracts were then obtained following the same procedure described above.

Locust behavioral responses to PAN and video-tracking system

We performed behavioral assays with gregarious locusts in the fourth instar to determine whether PAN plays an attractive role in locust aggregation. We used a vertical airflow olfactometer similar to that described by Obeng-Ofori *et al.* (*46*), with some modifications. Briefly, two square pyramidal stainless steel funnels (base length of 28 cm) were embedded in an inverted fashion in a stainless steel table (100 cm × 60 cm). The funnels were separated by a distance of 2 cm. The bottom of each funnel was fitted with stainless steel plates of uniform sizes and lengths of 28 cm. The plates were perforated with small holes 2 mm in diameter and 5 mm apart. To delineate a behavioral observation arena, a plexiglass chamber (60 cm × 30 cm × 30 cm) was used to enclose the area between the two plates. The table was placed in an observation chamber (150 cm × 100 cm × 180 cm) with a ventilation system and with a video camera mounted on the ceiling. Six 22-W white fluorescent tubes located on the side walls provided uniform lighting. An air conditioner was used to maintain the temperature in the chamber at 30° ± 2°C at all times. Each funnel was connected by Tygon tubing [internal diameter (ID), 0.7 cm] to an air purification system consisting of a compressed air cylinder, a charcoal filter, and a molecular sieve filter. A flowmeter was used to maintain the rate of the airflow through each vertical funnel to one side (zone) of the arena at 300 ml min^{-1}. The behavioral apparatus thus provided two choices for the tested locusts: a clean vertical airstream in the control zone and a neighboring vertical stream suffused with synthetic chemical in the PAN zone. A gregarious nymph in the fourth instar was introduced into the arena through a small door in the middle of the plexiglas chamber and was allowed to spend 10 min in the olfactometer. Different doses of PAN in paraffin oil (5, 50, 500, and 5000 ng/10 μl; Merck) were applied in a series of behavioral assays. The dosages were determined and normalized on the basis of the SPME measurements of PAN released over 10 min from various densities of living locusts (one funnel containing 1, 10, 50, 100, or 200 gregarious individuals in the fourth instar) in one arena. The dose used in behavioral assays was expressed as the release rate of LM (1 LM = PAN emitted by one locust for 10 min), and because 5 ng of PAN in 10 μl of paraffin oil was equivalent to the release rate of 1 LM, 50 ng/10 μl ≈ 10 LM, 500 ng/10 μl ≈ 200 LM, and 5000 ng/10 μl ≈ 1000 LM. Diluted PAN was applied to a piece of filter paper (3 cm × 3 cm; Whatman No. 1) and placed in one funnel, whereas paraffin oil was applied as the control in the other funnel. After 10 individuals had been tested, the position of the two sides of the funnels was reversed to prevent positional bias. Then, the funnels were heated to 180°C for 2 hours to eliminate odor residues. Under each treatment dosage, 25 locusts successfully finished the dual-choice tests (n = 25).

Behavioral activity over a 10-min period was filmed at 25 fps (frames per second) by using a video camera (Panasonic, WV-CP600/CH; 704 pixels × 576 pixels, analog output; a 3.0- to 8-mm F1.0 varifocal lens) coupled with Video Recorder software (version 2, Noldus Information Technology). The videos were analyzed with EthoVision XT software (version 11.5, Noldus Information Technology) to enable objective measurements of the total distance moved (traveled distance, in centimeters) and the total time spent in each side (in seconds) without biasing the preferences of the locusts treated with different dosages of synthetic PAN and the control.

PAN biosynthesis in locusts

To confirm the biosynthetic steps involved in the conversion of phenylalanine to PAN in locusts, D_8-Phe was incorporated into (*Z*/*E*)-PAOx and PAN in dsGFP- or ds*CYP305M2*-injected gregarious locusts and untreated solitary locusts (Fig. 2G). D_8-Phe was injected at a dose of 35 μg per locust into the second ventral segments of the abdomens of fourth-instar nymphs at 48 hours after ecdysis. Gregarious locusts were obtained from colonies reared at a density of 100 individuals. After 3 hours of incubation under rearing conditions, deuterium-labeled compound products were extracted from the head integuments by using a previously described method. Then, the extracts were analyzed using the method described below.

Deuterium-labeled (*Z*)-PAOx was incorporated into PAN in dsGFP- or ds*CYP305M2*-injected gregarious and untreated solitary locusts (Fig. 2H). D_8-(*Z*)-PAOx was injected at a dose of 1 μg per locust into the second ventral segments of the abdomens of fourth-instar nymphs at 48 hours after ecdysis. Gregarious locusts were obtained from colonies reared at a density of 100 individuals. After 3 hours of incubation under rearing conditions, deuterium-labeled PAN was extracted from the head integuments following the method

described above. Then, the extracts were analyzed using the method described below.

HCN biosynthesis in locusts

To determine whether PAN can be converted to HCN in locusts, we investigated HCN production in the headspace of fourth-instar nymphs at 48 hours after ecdysis. Gregarious locusts were obtained from colonies reared at a density of 100 individuals. Five nymphs under different treatments were confined in hermetically sealed glass vials to enrich the headspace HCN for 30 min before headspace analysis by GC-MS. Three treatments were performed: (i) Sealed vials containing intact nymphs were incubated at the rearing temperature (30° ± 2°C) to simulate HCN production in intact living nymphs. (ii) Locusts subjected to "hold-hammering" by birds were obtained and placed in sealed vials for HCN accumulation to detect HCN production by attacked nymphs. The detailed definitions of bird attack behavior are given in the "Bird behavioral assays" section. (iii) In accordance with the availability of wild captured birds and the requirements for wildlife welfare set by AECIOZ, we used shaking disturbance to mimic bird attacks in the in vivo chemical conversion experiments. Sealed vials containing chemical-injected nymphs were shaken vigorously for 30 s by using a vortex mixer to mimic predator attacks and then incubated at rearing temperature. A clean glass vial without nymphs served as the control. PAN, (*Z*)-PAOx, or solvent control (5% EtOH) was injected at a dose of 1 μg per locust or 10 μl per locust (5% EtOH) into the second ventral segments of the abdomens of solitary nymphs. After 3.5 hours of incubation under rearing conditions, the HCN of shake-disturbed (SD) and chemical-supplemented solitary locusts was measured through GC-MS, as described below. dsGFP- or ds*CYP305M2*-injected gregarious locusts were prepared and subjected to shaking disturbance treatment and HCN measurement, as described above.

BA biosynthesis in locusts

To determine whether Phe can be converted to BA in response to disturbance in locusts, we investigated BA production in fourth-instar nymphs. Chemicals were extracted at 48 hours after ecdysis from the head integuments of dsGFP- or ds*CYP305M2*-injected gregarious and untreated solitary locusts in the fourth instar under intact undisturbed and SD conditions. Gregarious locusts were obtained from colonies reared at a density of 100 individuals. Five living nymphs were confined in a hermetically sealed glass vial (20-ml headspace vial, MicroLiter Analytical Supplies Inc., Suwanee, USA). Two treatments were performed to (i) measure BA production by living nymphs under the intact condition, with sealed vials containing nymphs being incubated for 5 min at the rearing temperature (30° ± 2°C), and (ii) mimic the effect of disturbance on BA production, with sealed vials containing nymphs being shaken vigorously for 30 s using a vortex mixer and being incubated for 4.5 min at rearing temperature. All insects were anesthetized with CO_2 and frozen-killed in a refrigerator. Then, they were dissected to obtain head integument samples. Samples were homogenized as described above and then diluted with ACN (sample:ACN = 1:4, v/v) for protein removal. After 1 min of mixing with a vortex mixer, samples were centrifuged at 13,000 rpm for 10 min at 4°C. The upper layers of the samples were transferred to 1.5-ml Eppendorf tubes and concentrated under N_2 to approximately 10 μl. Subsequently, the residues were resolubilized in 100 μl of MeOH (80%, v/v, with water) in insert tubes (150 μl) in 2-ml screw-cap vials (Waters Co., USA) with Teflon/rubber septa and stored at −20°C until HPLC analysis.

D_8-Phe was incorporated into BA in SD dsGFP- or ds*CYP305M2*-injected gregarious or untreated solitary locusts (Fig. 4D). D_8-Phe was injected at a rate of 35 μg per locust into the second ventral segments of the abdomens of fourth-instar nymphs at 48 hours after ecdysis. Gregarious locusts were obtained from colonies reared at a density of 100 individuals. After 3.5 hours of incubation under rearing conditions, nymphs were shaken vigorously for 30 s using a vortex mixer and incubated for 4.5 min at rearing temperature. Then, deuterium-labeled compound products in the headspace vials were extracted through the SPME method as previously described, and the extracts were analyzed through GC-MS method as described below.

Chemical analysis and quantification

We used the same protocol described by Wei *et al.* (*14*) to identify and quantify PAN and isotope BA in SPME samples and PAN, (*Z*)-phenylacetaldoxime (Z-PAOx), and isotope (*Z*)-PAOx in locust tissues, organs, and body fluids. Briefly, a Bruker GC system (456-GC) coupled with a triple quadrupole (TQ) mass spectrometer (Scion TQ MS/MS Inc., Germany) equipped with a nonpolar DB-1MS column (30 m × 0.25 mm ID × 0.25 μm film thickness; Agilent Technologies) was used. The oven initial temperature on the DB-1MS column was maintained at 40°C for 4 min and then increased to 120°C at a rate of 5°C min^{-1}, then to 160°C at a programmed rate of 10°C min^{-1}, and finally to 320°C at a rate of 40°C min^{-1}. The GC-MS/MS electron impact source was operated in MRM mode. The SPME fiber was injected into an inlet operated in splitless injection mode and held for 1 min. Crude hexane extract (1 μl) was injected into the front inlet that was being operated in splitless mode. The two quantitative ions, namely, the precursor and productions, of PAN, PAOx, BA, and their deuterium-labeled compounds are shown in table S3. Data were analyzed and processed using a Bruker chemical analysis MS workstation (MS Data Review, Data Process, version 8.0). Different dosages of synthetic PAN (1, 5, 10, 50, and 100 ng/μl in hexane) were used as external standards to develop standard curves for the quantification of PAN in SPME samples. 4Me-PAN was added to each sample as an internal standard for the quantification of PAN, (*E*/*Z*)-PAOx, BA, and their deuterium-labeled compounds in different tissues, organs, and body fluids. The same thermal program and MRM method were used.

Nuclear magnetic resonance (NMR) spectroscopy was performed on a Bruker Advance II 400 MHz NMR spectrometer (Bruker NMR Technology). The ^1H experiment was performed under standard conditions, with CDCl3 as a solvent. The chemical shifts of the ^1H NMR of synthetic (*E*/*Z*)-PAOx are described in fig. S15.

The HCN content of the headspace of the living locusts was measured using the same GC-MS system as described above. The initial oven temperature of the DB-1MS column was maintained at 35°C for 5 min and increased to 130°C for 2 min at a rate of 50°C min^{-1} and to 300°C for 2 min at a programmed rate of 50°C min^{-1}. The overall run time was 14.3 min. The RT of HCN was first confirmed as 1.18 min through the full-scan mode. The GC-MS/MS electron impact source was then operated in selected ion monitoring mode. At an HCN RT of 1.18, the peak area of ion 27 was used to quantify the HCN, and ion 26 was used as the confirmation signal (fig. S13). Headspace gas (500 μl) from a glass vial containing five living nymphs was extracted with a 1-ml headspace syringe (Zinsser, Northridge, USA) and injected into the front inlet operated in split mode (split rate, 1:1). We used synthetic MAN as the standard to identify and quantify HCN because the HCN standard compound

is not commercially available, and MAN is directly decomposed to HCN and BA in the GC-MS injection port (*26*). Samples were quantified with the external calibration curve of HCN. The average peak area of HCN is one-fourth that of the output of BA in the GC-MS chromatogram of standard MAN. This proportion approaches the ratio of equimolar quantities of HCN and BA. First, a stock solution of MAN was prepared at a concentration of 1 mg/ml. Second, stock solutions were diluted through gentle pipetting with hexane to a dosage series of 0.1, 1, 10, and 100 ng/μl that corresponds to an HCN dosage series of 0.02 to 20 ng/μl. The calibration curves of the relation between the peak areas of HCN ion 27 and the corresponding dosages were developed under the same GC-MS condition as described above. Last, the concentration of HCN in 500 μl of headspace gas (indicated in micrograms per milliliter) of one sample was converted into the concentration of parts per billion (ppbv) HCN in a glass vial containing five living nymphs by using the following equation described by Zain *et al.* (*47*): HCN concentration (ppbv) = (HCN per locust from GC-MS result × volume of nymphs in a glass vial)/headspace gas volume in a glass vial × 1.10 μg/m^3. In this equation, the average volumes of the headspace gas and nymphs were determined as 18 and 2 ml, respectively, by adding water into 20-ml vials (fig. S18), and 1.10 μg/m^3 was set as the conversion factor of HCN in air (*47*).

To detect and quantify the BA and MAN in the locusts, we analyzed crude MeOH samples by using an HPLC machine (Agilent 1200 HPLC systems, Agilent Technologies) equipped with an Acclaim 120 C18 column (5 μm 120 Å, 250 mm × 4.6 mm ID; Thermo Fisher Scientific). An autosampler with an injection volume of 10 μl was used for all samples. Throughout the HPLC program, the column was maintained at 25°C at a flow rate of 1 ml min^{-1}, with the following programmed gradient: eluent B, 0 min, 20%; 0 to 15 min, 20 to 100%; 15 to 30 min, 100%; postrun, 10 min 20% eluent B. ACN and water were used as eluents B and A, respectively. The overall run time was 40 min. The UV detection wavelength was 254 nm. Synthetic MAN (RT, 13.82 min) and BA (RT, 16.69 min) at different dosages (0.1, 1, 10, 100, and 1000 ng/10 μl of MeOH) were used as external standards for the development of standard curves and the quantification of compounds in the samples. The same HPLC program was used.

We used the GC-MS/MS MRM method described above to identify and quantify PAN or other major locust volatiles in SPME samples from PAN-perfumed solitary or ds*CYP305M2*-injected locusts or their hexane-perfumed control counterparts (figs. S9 and S10). To perfume the locusts and mealworms with PAN, we individually placed the insects in 10-ml screw-cap glass vials, where chemicals had evaporated from pieces of filter paper (1.5 cm × 1.5 cm) containing 100 ng of PAN in hexane or 10 μl of the hexane control. After 30 min of fumigation with the chemicals, the insects were subjected to SPME for volatile absorption and then to GC-MS MRM system for chemical analysis (fig. S11C). BA or phenol was applied to solitary locusts as described above (fig. S12).

Molecular mechanism underlying PAN biosynthesis

RNA-seq data analysis

We previously identified 122 P450 genes in the genome of the migratory locust (fig. S3) (*11*). To identify candidate P450 genes that catalyze PAN biosynthesis in locusts, we reanalyzed our RNA-seq developmental data for gregarious and solitary locusts in the first to fifth instar (*48*). Transcript levels were calculated on the basis of the reads/kilobase per million mapped reads criteria. The difference between the gregarious and solitary groups was represented by a *P* value. Significantly differentially expressed genes ($P < 0.05$) in each comparison were enriched. We also performed unsupervised hierarchical clustering using Clustal 3.0, which uses uncentered Pearson correlation and average linkage. We used Java TreeView software to present our results.

RNA isolation and qRT-PCR analysis

Samples of different tissues and organs of nymphal locusts were obtained as described above. Total RNA was extracted from each sample by using an RNeasy Mini kit (Qiagen, Hilden, Germany) in accordance with the manufacturer's instructions and digested for 15 min with deoxyribonuclease I (Qiagen, Hilden, Germany) to eliminate residual genomic DNA. RNA concentration was determined using an ND-1000 spectrophotometer (NanoDrop, Wilmington, DE, USA). RNA integrity was confirmed through 1% agarose gel electrophoresis.

Complementary DNA (cDNA) pools were reverse-transcribed from 2 μg of total RNA isolated from each sample and used as the template for quantification. We performed quantitative reverse transcription polymerase chain reaction (qRT-PCR) analysis by using a LightCycler 480 system (Roche, Mannheim, Germany). The reaction volumes contained 5 μl of SYBR Green I Master Mix (Roche, Mannheim, Germany), 1 μl of the cDNA template, 5 μmol of each primer, and 3 μl of deionized water. The thermal cycling program comprised an initial 10-min denaturation cycle at 95°C, followed by 45 cycles at 95°C for 10 s, 58°C for 10 s, and 72°C for 20 s. Amplification specificity was confirmed through melting curve analysis. Gene expression levels were normalized to *rp49* gene expression. Expression data were analyzed using the equation $2^{-\Delta\Delta Ct}$. Primers were designed using Primer 5.0 software and are listed in table S2.

CYP gene–RNAi construction

The dsRNAs of *CYP305M2* and three other candidate genes (Fig. 2C and fig. S4, A to C) were synthesized by using the T7 RiboMAX Express RNAi System (Promega, Madison, USA) in accordance with the manufacturer's instructions. dsRNA concentrations were determined with an ND-1000 spectrophotometer, and dsRNA quality was verified through 1% agarose gel electrophoresis. At 3 hours after ecdysis, gregarious fourth-instar nymphs were separately injected with 9 μg of dsGFP or dsRNAs into the second ventral segment of the abdomen. The injected gregarious locusts were returned to gregarious rearing cages (Perspex boxes, 15 cm × 15 cm × 11 cm). After 2 days, the effects of RNAi were determined through qRT-PCR, and PAN emissions were determined as described above. RNAi locusts were used for bird predation experiments as described below. The primers for dsRNA preparation were designed using Primer 5.0 software and are listed in table S2.

Western blot analysis

Locust head integuments (10 to 12 individuals per sample) were collected and homogenized in 1× phosphate-buffered saline (PBS) buffer [0.1 M phosphate buffer and 0.15 M NaCl (pH 7.4)] containing the phosphatase inhibitor PhosSTOP (Roche) and a proteinase inhibitor (CWBIO, China). Total protein content was examined using a bicinchoninic acid protein assay kit (Thermo Fisher Scientific). The extracts (100 μg) were reduced, denatured, and electrophoresed on an 8% sodium dodecyl sulfate (SDS)–polyacrylamide gel electrophoresis (PAGE) gel and then transferred to a polyvinylidene difluoride membrane (Millipore). The membrane was then cut into two pieces and separately incubated overnight at 4°C with specific antibodies against

the target protein (~130 kDa) or reference protein [~55 kDa, affinity-purified polyclonal rabbit antibody against CYP305M2, 1:200, Sigma-Aldrich; rabbit polyclonal antibody against glyceraldehyde-3-phosphate dehydrogenase (GAPDH) (*49*), 1:5000, CWBIO, China]. Goat anti-rabbit immunoglobulin G (IgG) was used as secondary antibody (1:10,000; CWBIO, China). Protein bands were detected via chemiluminescence (ECL kit, CWBIO, China; Fig. 2D). The band intensities of the blots were quantified densitometrically with Quantity One software.

Immunohistochemistry

To prepare the polyclonal antibody against CYP305M2, we first designed four polypeptides as antigens on the basis of the antigenic epitopes of CYP305M2. Antiserum was obtained from immunized rabbits and then purified through saturated ammonium sulfate precipitation and affinity chromatography (Beijing Protein Innovation Co. Ltd.). Polyclonal antibody titers were determined using enzyme-linked immunosorbent assay. Antibody specificity was confirmed using SDS-PAGE and Western blot analyses. Only one polypeptide could recognize CYP305M2 (55 KD) specifically. The expression levels of the target protein of the polyclonal antibody decreased in gregarious or solitary locusts after RNAi treatment. These results indicate that the polyclonal antibody against the CYP305M2 protein was produced successfully and can be used to detect CYP305M2 protein in locust tissues.

The head integument tissues of fourth-instar nymphs were fixed overnight in 4% paraformaldehyde, embedded in paraffin through a conventional method, and cut into 7-μm-thick slides. The paraffin-embedded tissue slides were deparaffinized in xylene and rehydrated in a gradient EtOH series. The slides were then incubated for 30 min in blocking buffer (5% bovine serum albumin in PBS) and incubated overnight at 4°C with the primary antibody against ds*CYP305M2*. The slides were then hybridized for 1 hour with the secondary antibody [Alexa Fluor 488 goat anti-rabbit IgG(H + L); 1:1000] at room temperature and finally stained for 5 min with Hoechst33342 (1:4000). Signals were detected using an LSM 710 confocal fluorescence microscope (Zeiss, Jena, Germany; Fig. 2G).

Bird behavioral assays

Attacking behaviors of the great tit

To observe attacking behaviors of the great tit, we used a Perspex cage (25 cm × 25 cm × 25 cm) as an observation chamber. We covered five sides of the six-sided chamber with white paper to prevent exposing the bird to environmental disturbance during the assays. The side of the chamber that faced a video camera (Panasonic, WV-CP600/CH, Japan) remained uncovered (movie S6). A great tit that had been fasted for 4 hours was released in the chamber. Next, a pair of solitary and gregarious locusts was introduced into the chamber. The behavioral activity of the great tit over a 5-min period was filmed at 25 fps by using the video camera. A researcher played back the videos to analyze the attacking behaviors exhibited by the bird. The great tit exhibited two distinct attacking behaviors when it encountered a locust. The bird began attacking by showing "seizing and dropping" behavior, wherein the bird used its beak to seize and drop a locust several times in quick succession (means ± SEM, 7.48 ± 1.6 times, n = 8 birds). Then, the locust was killed through hold-hammering behavior. In this behavior, the bird first held the body of the prey under the tarsus and then used its beak to strike the locust several times (means ± SEM, 13.8 ± 1.3 times, n = 8 birds) until the head integument and tergum of the locust ruptured and the locust was ready for eating (movie S6). The handling time before the prey was ready for eating was approximately 30 s (means ± SE, 33.5 ± 3.5 s, n = 8 birds). These behaviors are our rationale for using shaking disturbance (30-s duration on a vortex mixer) to mimic predator attacks.

We used the same setup to obtain predator-attacked locusts for HCN measurements. We used a video camera to monitor the attacking behaviors of the birds. We used forceps to collect locusts that had been handled by the bird at the end of the hold-hammering stage. The injured locust was placed in a sealed vial for HCN accumulation. A new locust was then offered successively until the bird refused to attack further offerings. Six birds were used in this experiment.

Dual-choice experiments

To assess whether the great tit preferentially selects and preys on solitary locusts over gregarious locusts in the presence or absence of visual cues, we offered a series of paired living solitary and gregarious fourth-instar locusts to great tits under light and dark conditions. The birds were deprived of diet for 4 hours before testing. The birds were then initially presented with a mealworm to trigger hunger. Whenever a bird attempted to approach and attack the mealworm, the mealworm was withdrawn, and the bird was regarded as hungry without neophobic reaction (fig. S19). The bird was then subjected to formal testing. A pair of solitary and gregarious locusts were offered to a bird that was confined in a birdcage (19 cm × 13 cm × 12 cm; a topless birdcage was used in the dark). Each locust was weighed to determine initial biomass and then suspended by sewing threads fixed on two ends of a bamboo stick to eliminate the effect of the different locomotive capabilities of birds on the catchability of solitary and gregarious locusts (fig. S8 and movies S1 and S2). We then recorded the attacking and feeding behaviors of the bird on the pair of prey items under light and dark conditions by using a digital video camera (4K FDR-AX30, Sony, Japan) operated at 25 fps in normal mode or night-shot mode. Each assay lasted for 5 min. After the assay, we weighed the biomass of each prey, including the remaining uneaten body parts of the victims. A new pair of locusts was then offered successively until the bird refused to attack further offerings. The positions of solitary and gregarious locusts offered to each bird were reversed after each assay to avoid positional bias. On average, three to five pairs of locusts were offered before the bird ceased attacking. We tested 10 birds under light conditions and 8 birds under dark conditions. We calculated the average first-choice rate of birds for either solitary or gregarious locusts (under light, n = 10; under dark, n = 8). The injury rates (the incidence of each locust injured by birds) and consumption rates (the percentage of the total biomass of each locust lost by bird feeding on each paired offering) were determined (fig. S8, A and B).

To investigate whether PAN load influences choice and predation by great tits, we subjected fourth-instar nymphs with or without PAN treatment to a series of dual-choice and predation tests under light conditions following the same protocol mentioned above. The treatments of the paired offerings included solitary + hexane versus solitary + PAN locusts, dsGFP-injected locusts versus ds*CYP305M2*-injected locusts, and hexane + ds*CYP305M2*–injected locusts versus PAN + ds*CYP305M2*–injected locusts (Fig. 3 and fig. S20). On average, three to five paired locusts were offered to one bird (fig. S20). In all of these dual-choice experiments, 8 to 12 birds successfully applied their choices to a series of paired locusts. To determine whether birds also exhibited negative responses to PAN-perfumed mealworms or BA- or phenol-perfumed solitary locusts, we applied chemicals on mealworms or solitary locusts following the same protocol as that

followed for PAN treatment. After 30 min of fumigation with PAN, BA, phenol, or the hexane control in vials, paired mealworms (in a group of five individuals per treatment) or solitary locusts were offered to hungry birds (figs. S11B and S12). In the dual-choice tests, six to eight birds successfully applied their choices to a series of paired offerings. We calculated the first-choice rate, injury rate, and consumption rate under each treatment (Fig. 3 and figs. S11 and S12).

Data analysis

The SPSS 17.0 (SPSS Inc., Chicago, IL, USA) statistical analysis software was used to process all data. The behavioral data of locusts and birds were analyzed for statistical significance using Wilcoxon signed rank test (n = 25 locusts for each dosage; n = 8 to 12 birds for each paired locust; means ± SEM). Data of PAN, (*E*/*Z*)-PAOx, BA, and their deuterium-labeled analogs between or among the different treatments were analyzed statistically using the Shapiro-Wilk test to assess for normality and equal variance test for same variance, followed by a two-tailed Student's t test or ANOVA with the following Tukey honestly significant difference (HSD) post hoc test. Otherwise, a Mann-Whitney U test, Wilcoxon rank sum test, or Kruskal-Wallis one-way ANOVA on ranks was used as appropriate. When a multiple comparison test was needed, the Tukey's multiple comparisons test was used. The same method was applied to determine the statistical significance of the BA and the HCN productions between or among treatments in locusts.

SUPPLEMENTARY MATERIALS

Supplementary material for this article is available at http://advances.sciencemag.org/cgi/content/full/5/1/eaav5495/DC1

Supplementary Text

Fig. S1. PAN accumulation in tissues, organs, and body fluids of gregarious locusts.

Fig. S2. PAN dominates the six major volatile compounds released in headspace and dissolved in hemolymph of fourth-instar gregarious locusts

Fig. S3. Cytochrome (CYP) P450 gene transcriptomic analyses in whole body of gregarious and solitary locusts from first- to fifth-instar nymphs.

Fig. S4. Knockdown of three putative CYP genes by RNAi.

Fig. S5. Alignment of amino acid sequences of LmCYP305M2 (*LM16181* shown in fig. S3B) with other five members in CYP305A subfamily of other insect species.

Fig. S6. *CYP305M2* gene expression levels in different tissues and organs of fifth-instar gregarious locusts.

Fig. S7. The histological localization of CYP305M2 in tissue slides of head integument of dsGFP.

Fig. S8. Gregarious locusts are distasteful to the great tit (*P. major*).

Fig. S9. Major volatile components in the headspaces of hexane- and PAN-treated solitary locusts.

Fig. S10. Comparison of major volatile components in headspaces between dsGFP- and *dsCYP305M2*-injected locusts or between hexane-treated and PAN-treated *dsCYP305M2*-injected locusts.

Fig. S11. Perfuming beetle mealworm (*T. molitor*) with PAN increased the larval survivorship.

Fig. S12. Perfuming fourth-instar solitary locusts (S4) with BA or phenol did not affect the bird selection and predation.

Fig. S13. Extracted-ion GC-MS chromatograms of ion 26 of synthetic HCN and HCN in headspaces of locusts.

Fig. S14. HPLC chromatograms of BA in the head integuments of fourth-instar gregarious (G) and solitary (S) locusts.

Fig. S15. Confirmation of synthetic (*E*/*Z*)-PAOx with NMR and GC-MS.

Fig. S16. Confirmation of synthetic D8-(*E*/*Z*)-PAOx with GC-MS.

Fig. S17. HPLC chromatogram of D_8-(*E*/*Z*)-PAOx.

Fig. S18. Measurement of the average volumes of headspace gas and locusts in a hermetically sealed glass vial (20 ml).

Fig. S19. Bird hungry and neophobic test before experiments.

Fig. S20. PAN load of locusts influences predation by the great tit.

Table S1. (*E*/*Z*)-PAOx in hexane extracts of tissues, organs, and body fluids of gregarious fourth-instar locusts.

Table S2. Primer sequences used for PCR amplification and the dsRNA synthesis of the putative genes in PAN biosynthetic pathway.

Table S3. MRM precursor and product ions and their collision energies (CE) of compounds.

Movie S1. Video clip showing a bird preferring to attack a solitary fourth-instar locust as its first choice under light condition.

Movie S2. Video clip showing a bird preferring to attack a solitary fourth-instar locust (S4) as its first choice under dark condition in a topless birdcage.

Movie S3. Video clip demonstrating the effect of PAN supplementation on bird choice and predation on solitary locusts.

Movie S4. Video clip shows that great tits preferentially attacked and consumed a ds*CYP305M2*-injected gregarious locust (RNAi) over a dsGFP-injected gregarious locust (GFP).

Movie S5. Video clip showing the effect of PAN supplementation on bird choice and predation on ds*CYP305M2*-injected gregarious locust.

Movie S6. Video clip showing bird-attacking behaviors in an observation chamber.

REFERENCES AND NOTES

1. J. K. Parrish, L. Edelstein-Keshet, Complexity, pattern, and evolutionary trade-offs in animal aggregation. *Science* **284**, 99–101 (1999).
2. M. Riipi, R. V. Alatalo, L. Lindström, J. Mappes, Multiple benefits of gregariousness cover detectability costs in aposematic aggregations. *Nature* **413**, 512–514 (2001).
3. J. L. Gittleman, P. H. Harvey, Why are distasteful prey not cryptic? *Nature* **286**, 149–150 (1980).
4. G. D. Ruxton, T. N. Sherratt, Aggregation, defence and warning signals: The evolutionary relationship. *Proc. Biol. Sci.* **273**, 2417–2424 (2006).
5. B. Sillen-Tullberg, O. Leimar, The evolution of gregariousness in distasteful insects as a defense against predators. *Am. Nat.* **132**, 723–734 (1988).
6. G. D. Ruxton, T. N. Sherratt, M. P. Speed, *Avoiding Attack: The Evolutionary Ecology of Camouflage, Warning Signals and Mimicry* (Oxford Univ. Press Inc., 2004).
7. J. D. Blount, M. P. Speed, G. D. Ruxton, P. A. Stephens, Warning displays may function as honest signals of toxicity. *Proc. Biol. Sci.* **276**, 871–877 (2009).
8. E. Despland, Diet breadth and anti-predator strategies in desert locusts and other orthopterans. *J. Orthop. Res.* **14**, 227–233 (2005).
9. G. A. Sword, S. J. Simpson, O. T. M. El Hadi, H. Wilps, Density–dependent aposematism in the desert locust. *Proc. Biol. Sci.* **267**, 63–68 (2000).
10. X. Wang, X. Fang, P. Yang, X. Jiang, F. Jiang, D. Zhao, B. Li, F. Cui, J. Wei, C. Ma, Y. Wang, J. He, Y. Luo, Z. Wang, X. Guo, W. Guo, X. Wang, Y. Zhang, M. Yang, S. Hao, B. Chen, Z. Ma, D. Yu, Z. Xiong, Y. Zhu, D. Fan, L. Han, B. Wang, Y. Chen, J. Wang, L. Yang, W. Zhao, Y. Feng, G. Chen, J. Lian, Q. Li, Z. Huang, X. Yao, N. Lv, G. Zhang, Y. Li, J. Wang, J. Wang, B. Zhu, L. Kang, The locust genome provides insight into swarm formation and long-distance flight. *Nat. Commun.* **5**, 2957 (2014).
11. T. Eisner, R. Grant, Toxicity, odor aversion, and "olfactory aposematism". *Science* **213**, 476 (1981).
12. A. L. Deng, B. Torto, A. Hassanali, E. E. Ali, Effects of shifting to crowded or solitary conditions on pheromone release and morphometrics of the desert locust, *Schistocerca gregaria* (Forskål) (Orthoptera: Acrididae). *J. Insect Physiol.* **42**, 771–776 (1996).
13. M. P. Pener, S. J. Simpson, Locust phase polyphenism: An update. *Adv. Insect Physiol.* **36**, 1–272 (2009).
14. J. Wei, W. Shao, X. Wang, J. Ge, X. Chen, D. Yu, L. Kang, Composition and emission dynamics of migratory locust volatiles in response to changes in developmental stages and population density. *Insect Sci.* **24**, 60–72 (2017).
15. M. Kai, U. Effmert, G. Berg, B. Piechulla, Volatiles of bacterial antagonists inhibit mycelial growth of the plant pathogen *Rhizoctonia solani*. *Arch. Microbiol.* **187**, 351–360 (2007).
16. R. R. Junker, C. Loewel, R. Gross, S. Dötterl, A. Keller, N. Blüthgen, Composition of epiphytic bacterial communities differs on petals and leaves. *Plant Biol.* **13**, 918–924 (2011).
17. T. Bellas, B. Hölldobler, Constituents of mandibular and Dufour's glands of an australian *Polyrhachis* weaver ant. *J. Chem. Ecol.* **11**, 525–538 (1985).
18. S. Irmisch, A. Clavijo McCormick, J. Günther, A. Schmidt, G. A. Boeckler, J. Gershenzon, S. B. Unsicker, T. G. Köllner, Herbivore-induced poplar cytochrome P450 enzymes of the CYP71 family convert aldoximes to nitriles which repel a generalist caterpillar. *Plant J.* **80**, 1095–1107 (2014).
19. K. Seidelmann, K. Warnstorff, H.-J. Ferenz, Phenylacetonitrile is a male specific repellent in gregarious desert locusts, *Schistocerca gregaria*. *Chemoecology* **15**, 37–43 (2005).
20. S. S. Duffey, G. H. N. Towers, On the biochemical basis of HCN production in the millipede *Harpaphe haydeniana* (Xystodesmidae: Polydesmida). *Can. J. Zool.* **56**, 7–16 (1978).
21. M. v. Ohlen, A.-M. Herfurth, U. Wittstock, in *Herbivores*, V. D. C. Shields, Ed. (InTech, 2017), chap. 2, pp. 29–57.
22. K. Seidelmann, H. Weinert, H.-J. Ferenz, Wings and legs are production sites for the desert locust courtship-inhibition pheromone, phenylacetonitrile. *J. Insect Physiol.* **49**, 1125–1133 (2003).
23. M. Zagrobelny, S. Bak, B. L. Møller, Cyanogenesis in plants and arthropods. *Phytochemistry* **69**, 1457–1468 (2008).
24. U. Wittstock, B. A. Halkier, Cytochrome P450 CYP79A2 from *Arabidopsis thaliana* L. catalyzes the conversion of L-phenylalanine to phenylacetaldoxime in the biosynthesis of benzylglucosinolate. *J. Biol. Chem.* **275**, 14659–14666 (2000).

25. S. Irmisch, A. C. McCormick, G. A. Boeckler, A. Schmidt, M. Reichelt, B. Schneider, K. Block, J.-P. Schnitzler, J. Gershenzon, S. B. Unsicker, T. G. Köllner, Two herbivore-induced cytochrome P450 enzymes CYP79D6 and CYP79D7 catalyze the formation of volatile aldoximes involved in poplar defense. *Plant Cell* **25**, 4737–4754 (2013).
26. T. Yamaguchi, K. Yamamoto, Y. Asano, Identification and characterization of CYP79D16 and CYP71AN24 catalyzing the first and second steps in L-phenylalanine-derived cyanogenic glycoside biosynthesis in the Japanese apricot, *Prunus mume* Sieb. et Zucc. *Plant Mol. Biol.* **86**, 215–223 (2014).
27. T. Yamaguchi, K. Noge, Y. Asano, Cytochrome P450 CYP71AT96 catalyses the final step of herbivore-induced phenylacetonitrile biosynthesis in the giant knotweed, *Fallopia sachalinensis*. *Plant Mol. Biol.* **91**, 229–239 (2016).
28. Y. Asano, Y. Kato, Z-phenylacetaldoxime degradation by a novel aldoxime dehydratase from *Bacillus* sp. strain OxB-1. *FEMS Microbiol. Lett.* **158**, 185–190 (1998).
29. H.-J. Ferenz, K. Seidelmann, Pheromones in relation to aggregation and reproduction in desert locusts. *Physiol. Entomol.* **28**, 11–18 (2003).
30. M. Dadashipour, Y. Ishida, K. Yamamoto, Y. Asano, Discovery and molecular and biocatalytic properties of hydroxynitrile lyase from an invasive millipede, *Chamberlinius hualienensis*. *Proc. Natl. Acad. Sci. U.S.A.* **112**, 10605–10610 (2015).
31. T. Yamaguchi, Y. Kuwahara, Y. Asano, A novel cytochrome P450, CYP3201B1, is involved in (*R*)-mandelonitrile biosynthesis in a cyanogenic millipede. *FEBS Open Bio* **7**, 335–347 (2017).
32. A. Gosler, P. Clement, in *Handbook of the Birds of the World. Volume 12: Picathartes to Tits and Chickadees*, J. del Hoyo, A. Elliott, D. Christie, Eds. (Lynx Edicions, 2007), chap. 662–709.
33. K. Noge, S. Tamogami, Herbivore-induced phenylacetonitrile is biosynthesized from de novo-synthesized L-phenylalanine in the giant knotweed, *Fallopia sachalinensis*. *FEBS Lett.* **587**, 1811–1817 (2013).
34. B. Torto, D. Obeng-Ofori, P. G. N. Njagi, A. Hassanali, H. Amiani, Aggregation pheromone system of adult gregarious desert locust *schistocerca gregaria* (forskal). *J. Chem. Ecol.* **20**, 1749–1762 (1994).
35. J. Potter, R. L. Smith, A. M. Api, An assessment of the release of inorganic cyanide from the fragrance materials benzyl cyanide, geranyl nitrile and citronellyl nitrile applied dermally to the rat. *Food Chem. Toxicol.* **39**, 147–151 (2001).
36. G. Giordano, M. Carbone, M. L. Ciavatta, E. Silvano, M. Gavagnin, M. J. Garson, K. L. Cheney, I. W. Mudianta, G. F. Russo, G. Villani, L. Magliozzi, G. Polese, C. Zidorn, A. Cutignano, A. Fontana, M. T. Ghiselin, E. Mollo, Volatile secondary metabolites as aposematic olfactory signals and defensive weapons in aquatic environments. *Proc. Natl. Acad. Sci. U.S.A.* **114**, 3451–3456 (2017).
37. C. G. Longson, J. M. P. Joss, Optimal toxicity in animals: Predicting the optimal level of chemical defences. *Funct. Ecol.* **20**, 731–735 (2006).
38. L. Lindström, C. Rowe, T. Guilford, Pyrazine odour makes visually conspicuous prey aversive. *Proc. Biol. Sci.* **268**, 159–162 (2001).
39. P. J. Gullan, P. S. Cranston, *The Insects: An Outline of Entomology* (Wiley-Blackwell, 2014).
40. R. M. Gleadow, B. L. Møller, Cyanogenic glycosides: Synthesis, physiology, and phenotypic plasticity. *Annu. Rev. Plant Biol.* **65**, 155–185 (2014).
41. A. Brückner, G. Raspotnig, K. Wehner, R. Meusinger, R. A. Norton, M. Heethoff, Storage and release of hydrogen cyanide in a chelicerate (*Oribatula tibialis*). *Proc. Natl. Acad. Sci. U.S.A.* **114**, 3469–3472 (2017).
42. W. A. Shear, The chemical defenses of millipedes (diplopoda): Biochemistry, physiology and ecology. *Biochem. Syst. Ecol.* **61**, 78–117 (2015).
43. F. O. Albrecht, M. Verdier, R. E. Blackith, Maternal control of ovariole number in the progeny of the migratory locust. *Nature* **184**, 103–104 (1959).
44. B. P. Uvarov, *Grasshoppers and Locusts: A Handbook of General Acridology*. *Anatomy, Physiology, Development, Phase Polymorphism, Introduction to Taxonomy* (Cambridge Univ. Press, 1966), vol. 1.
45. A. Niassy, B. Torto, P. G. N. Njagi, A. Hassanali, D. Obeng-Ofori, J. N. Ayertey, Intra- and interspecific aggregation responses of *Locusta migratoria migratorioides* and *Schistocerca gregaria* and a comparison of their pheromone emissions. *J. Chem. Ecol.* **25**, 1029–1042 (1999).
46. D. Obeng-Ofori, B. Torto, A. Hassanali, Evidence for mediation of two releaser pheromones in the aggregation behavior of the gregarious desert locust, *Schistocerca gregaria* (forskal) (Orthoptera: Acrididae). *J. Chem. Ecol.* **19**, 1665–1676 (1993).
47. S. M. Sayed Mohamed Zain, R. Shaharudin, M. A. Kamaluddin, S. F. Daud, Determination of hydrogen cyanide in residential ambient air using SPME coupled with GC–MS. *Atmos. Pollut. Res.* **8**, 678–685 (2017).
48. S. Chen, P. Yang, F. Jiang, Y. Wei, Z. Ma, L. Kang, De novo analysis of transcriptome dynamics in the migratory locust during the development of phase traits. *PLOS ONE* **5**, e15633 (2010).
49. Y. Wang, P. Yang, F. Cui, L. Kang, Altered immunity in crowded locust reduced fungal (*Metarhizium anisopliae*) pathogenesis. *PLOS Pathog.* **9**, e1003102 (2013).

Acknowledgments: We thank D. Nelson for naming cytochrome P450 gene and B. Smith for English editing and comments. The supply of bird rearing room and experimental place was supported by F. Lei (IOZ, CAS). We also thank Y. Wang for providing GAPDH antibody in Western blot and W. Li for HPLC assistance. **Funding:** This work was supported by the Strategic Priority Research Program of the Chinese Academy of Sciences (grants XDB11050600 and XDB11010200) and the National Nature Science Foundation of China (31210103915).
Author contributions: J.W., X.W., and L.K. conceived and designed the experiments. J.W. performed the behavioral tests and chemical analyses. W.S. and M.C. conducted Western blot analysis and gene expressions. L.C. and J.G. provided the analytical tools. J.W., W.S., M.C., and P.Y. analyzed the data. J.W., X.W., and L.K. wrote the manuscript. **Competing interests:** The authors declare that they have no competing interests. **Data and materials availability:** All the data needed to understand and assess the conclusions of this research are available in the main text, Supplementary Materials, and GenBank (accession number MG571525). Additional data related to this paper may be requested from the authors.

Submitted 28 September 2018
Accepted 11 December 2018
Published 23 January 2019
10.1126/sciadv.aav5495

Citation: J. Wei, W. Shao, M. Cao, J. Ge, P. Yang, L. Chen, X. Wang, L. Kang, Phenylacetonitrile in locusts facilitates an antipredator defense by acting as an olfactory aposematic signal and cyanide precursor. *Sci. Adv.* **5**, eaav5495 (2019).

ScienceAdvances

Phenylacetonitrile in locusts facilitates an antipredator defense by acting as an olfactory aposematic signal and cyanide precursor

Jianing Wei, Wenbo Shao, Minmin Cao, Jin Ge, Pengcheng Yang, Li Chen, Xianhui Wang and Le Kang

Sci Adv **5** (1), eaav5495.
DOI: 10.1126/sciadv.aav5495